Am J Transl Res 2026;18(2):1705-1718
www.ajtr.org /ISSN:1943-8141/AJTR0169099

Original Article

Propofol decreases the resistance of neutrophils to Candida albicans by inhibiting ferroptosis and the cGAS-STING pathway

Tingting Wei[1*], Lindong Cheng[2*], Ping Li[3*], Jing Huang[4], Yi Wang[2], Ning Ma[5], Liangqing Lin[6], Lin Zhou[1]

[1]Department of Laboratory Medicine, Shanghai Changzheng Hospital, Naval Medical University, 415 Fengyang Road, Shanghai 200003, China; [2]Department of Anesthesiology, Naval Medical University, Shanghai 200433, China; [3]Department of Anesthesiology, Shanghai Changhai Hospital, Naval Medical University, 168 Changhai Road, Shanghai 200433, China; [4]Graduate School, Wannan Medical College, Wuhu 241000, Anhui, China; [5]Department of Clinical Laboratory, 905th Hospital of PLA, Shanghai 200052, China; [6]Department of Anesthesiology, The First Hospital of Putian City, Teaching Hospital of Fujian Medical University, 449 Nanmen West Road, Putian 351100, Fujian, China. [*]Equal contributors.

Received September 30, 2025; Accepted February 4, 2026; Epub February 15, 2026; Published February 28, 2026

Abstract: *Candida albicans* (*C. albicans*) is a significant fungal pathogen responsible for serious infections, especially in immunocompromised persons. Neutrophils are crucial for innate protection against fungal infections. The anesthetic propofol influences immunological activities, however its impact on neutrophil antifungal activity remains ambiguous. This study examined the effects of propofol on neutrophil responses in humans and mice to *C. albicans* and evaluated clinical consequences. In vitro, human neutrophils pretreated with propofol exhibited decreased fungal eradication. Propofol diminished glutathione levels, elevated malondialdehyde and ferrous iron concentrations, and inhibited the activation of the cyclic GMP-AMP synthase (cGAS) - stimulator of interferon genes (STING) pathway as well as ferroptosis indicators. In *C. albicans*-infected mice, propofol diminished renal inflammation, although augmented fungal load and decreased pro-inflammatory cytokines. An analysis of 836 ICU patients with fungal infections from the MIMIC-IV database indicated that propofol-treated patients experienced prolonged hospital stays compared to untreated controls, with no change in fatality rates. Propofol hinders neutrophil clearance of *C. albicans* by obstructing cGAS-STING signaling and ferroptosis.

Keywords: Propofol, neutrophils, *Candida albicans*, ferroptosis, cGAS-STING

Introduction

Candida albicans (*C. albicans*), a prevalent commensal organism within the cutaneous and intestinal microbiota, normally colonizes the epithelial surfaces of healthy individuals [1, 2]. It may overgrow and trigger invasive fungal infections when host immune defenses are compromised [3]. As the primary etiological agent of invasive candidiasis, *C. albicans* causes - 400,000 annual life-threatening systemic infections in severely immunocompromised patients worldwide and is among the leading causes of hospital-acquired infections [4-6]. Upon invasion, the host initiates a diverse array of sophisticated immune mechanisms to control and eliminate this pathogen, among which innate immunity acts as the body's first line of defense [7-9]. The control and resolution of *C. albicans* infection primarily rely on coordinated interactions between multiple immune cell types - including dendritic cells (DCs), macrophages, neutrophils, and natural killer cells - and the cytokines secreted by these cells [10-13]. Neutrophils, as the primary immune effectors against *C. albicans*, eliminate this fungus primarily through four key mechanisms: phagocytosis, reactive oxygen species (ROS) production, degranulation, and the formation of neutrophil extracellular traps (NETs) [14, 15].

Propofol, a commonly used intravenous anesthetic for surgical anesthesia and ICU sedation, exerts immunomodulatory effects that disrupt

https://doi.org/10.62347/JAUQ9954

macrophage functions, including chemotaxis, oxidative burst, and phagocytosis [16, 17]. It also impacts the production of proinflammatory cytokines including tumor necrosis factor-α (TNF-α), interleukin-1β (IL-1β), and interleukin-6 (IL-6) in macrophages, and suppresses phagocytosis and apoptosis [18]. However, the impact of propofol on neutrophils' antifungal activity against *C. albicans* remains unclear.

Ferroptosis, a regulated cell death distinct from apoptosis and necrosis, is initiated by intracellular lipid reactive oxygen species (L-ROS) generated through the activation of enzymes involving iron and polyunsaturated fatty acids (PUFA) [19, 20]. Neutrophil ferroptosis plays a key role in various pathological conditions [21, 22]. It clears phagocytosis-resistant pathogens during infection [23], modulates inflammation by amplifying and resolving immune responses [24], and mitigates autoimmune diseases by eliminating hyperactive cells [25]. In *C. albicans* infection, ferroptosis may enhance antifungal immunity through the release of ROS and inflammatory mediators upon cell membrane damage [26]. However, excessive ferroptosis can cause collateral host tissue damage [27]. Thus, neutrophil ferroptosis has a dual impact on *C. albicans* infection - facilitating pathogen control while potentially inducing tissue injury. Comprehensive understanding of its mechanisms is crucial for developing targeted antifungal therapies.

The cyclic GMP-AMP synthase (cGAS) - stimulator of interferon genes (STING) signaling pathway is a crucial component of the innate immune system that detects cytosolic DNA and triggers downstream immune responses. Recent studies have provided compelling evidence for the critical role of the cGAS-STING pathway in fungal infections, particularly in keratitis models. In fungal infections such as *Aspergillus fumigatus* keratitis, the cGAS-STING pathway is essential for mediating inflammatory responses and autophagy. Specifically, the knockdown of cGAS results in a reduction of pro-inflammatory cytokines induced by *Aspergillus fumigatus*, whereas the restoration of cGAS activity can reinitiate the inflammatory response [28]. In the pathogenesis of *C. albicans* keratitis, inhibition of this pathway exacerbates the disease, as indicated by elevated clinical scores, increased fungal burden, and heightened inflammatory responses [29]. Furthermore, in the context of immunosenescence, ceramide can modulate the activation of this pathway by regulating mitochondrial permeability, thereby inhibiting the delayed apoptosis of neutrophils [30]. This suggests that the pathway is not only involved in immune responses to infection, but may also play a role in regulating the aging process of immune cells. Given the importance of this pathway in antifungal immunity, understanding how clinical interventions might modulate cGAS-STING signaling is crucial, particularly in the context of neutrophil function.

This study aimed to identify the mechanisms underlying propofol-mediated regulation of *C. albicans* infection and to investigate whether propofol influences neutrophils' killing capacity against *C. albicans* by regulating neutrophil ferroptosis.

Materials and methods

Mice

C57BL/6J mice aged 6-8 weeks were purchased from Shanghai Laboratory Animal Center. All experimental procedures were performed under the standards of the Association for Assessment and Accreditation of Laboratory Animal Care (AAALAC). This project was approved by the Ethics Committee of the Naval Military Medical University.

Culture and heat inactivation of C. albicans strain SC5314

C. albicans strain SC5314 was provided by Dr. N. Ma. *C. albicans* colonies were grown overnight at 30°C in yeast extract peptone dextrose (YPD) medium, then transferred to a 37°C environment in YPD with 10% FBS for 3 hours to induce hyphae formation. Yeast cells were washed three times and resuspended in phosphate-buffered saline (PBS) buffer, then incubated at 65°C for 1 hour to obtain heat-killed *C. albicans* (HKCA).

Systemic C. albicans infection

For each infection, a colony was cultured in YPD medium at 30°C for 24 hours, then washed with PBS and diluted to 4×10^5 cells/ml. These yeast cells were injected into 6-8-week-old

mice via the tail vein. The mice's body weight was monitored daily. At the experimental endpoint (1 or 5 days post-infection), mice were euthanized by exposure to a gradually increasing concentration of carbon dioxide (CO_2), followed by cervical dislocation as a secondary method to ensure death. Subsequently, kidneys, livers, lungs, and spleens were collected to measure fungal burden. Tissues were homogenized, diluted, and spread on YPD agar plates to count fungal CFUs after 24 hours [31].

Histopathology

The kidneys were preserved in 4% paraformaldehyde for 2-3 days before being sent to Servicebio (Wuhan, China) for paraffin embedding, sectioning, and staining.

Purification of peripheral blood polymorphonuclear neutrophils (PMNs)

Human peripheral blood was provided by the 905th Hospital of PLA. Human PMNs were isolated using density gradient centrifugation with 3% Dextran and Ficoll-Hypaque. The PMN pellet was then resuspended at 1×10^6 cells/ml in DMEM with 10% FBS, 1% glutamine, and 1% penicillin/streptomycin [32].

Cell viability

Cell viability was assessed using the CCK-8 assay. Neutrophils (1×10^4 cells/well) or *C. albicans* were seeded in 96-well plates and incubated overnight to allow cell attachment. Following overnight incubation, cultures were exposed to propofol at different concentrations for 3, 6, or 12 hours. CCK-8 reagent (10 μL; Dojindo, China) was then added to each well, and plates were incubated for an additional 2 hours at 37°C. Cell viability was determined by measuring optical density at 450 nm using a microplate reader (Thermo-Fisher Scientific, USA).

Enzyme-linked immunosorbent assay (ELISA)

The levels of glutathione (GSH), malondialdehyde (MDA), and Fe^{2+} in cell culture supernatants, as well as the levels of TNF-α, IL-1β, and IL-6, were measured using ELISA Kits (Elabscience).

Western blot analysis

Protein samples were separated on 10% SDS-PAGE gels, transferred to PVDF membranes, blocked, and incubated overnight at 4°C with a primary antibody. A HRP-conjugated secondary antibody was applied for two hours at room temperature, followed by ECL reagent for visualization. Protein expressions were analyzed with ImageJ software (n = 3).

In vitro killing assay

For the in vitro fungal killing assay, PMNs at a concentration of 5×10^5 cells per well were incubated with *C. albicans* at a multiplicity of infection (MOI) of 3 for 3 hours. Following the co-culture, the cells underwent washing with PBS and were subsequently resuspended in a medium containing 30 μg/mL amphotericin B. The culture was then maintained for an additional 3 hours at 37°C. After a subsequent washing step, the cells were lysed using 0.02% Triton X-100. The suspension was diluted 1:1000 and spread on YPD AGAR plates. Bactericidal efficacy was determined by counting *C. albicans* colonies after 24 h of incubation at 37°C. Treated cells were seeded in 12-well plates and incubated with *C. albicans* at a MOI of 1:50 overnight at 37°C. Subsequently, the cells were fixed with 4% paraformaldehyde and stained with crystal violet. The extent of fungal growth was quantified using ImageJ [33].

Data extraction

Intensive Care Unit (ICU) patients with fungal infections were identified from the Medical Information Mart for Intensive Care (MIMIC)-IV 2.0 database using ICD-10 code B37. The inclusion criteria for the study were as follows: (1) adults aged 18-89 years; and (2) the first recorded microbial event of a fungal infection. The exclusion criteria included: (1) patients younger than 18 years; (2) patients with incomplete or missing clinical data; and (3) patients identified with respiratory specimens as the type of infection. The primary outcome measure was all-cause mortality. Patient data were systematically collected, encompassing the following categories: (1) demographic characteristics, including age and weight; (2) vital signs, such as heart rate, body temperature, blood oxygen saturation (SpO_2), respiratory rate (bpm), and body temperature; (3) laboratory results, comprising total bilirubin, anion gap, creatinine, blood urea nitrogen (BUN), white blood cells, glucose, hemoglobin, bicarbonate, creatinine, sodium, partial thromboplastin time (PTT), prothrombin time (PT), and international

normalized ratio (INR); (4) illness severity scores, including the Glasgow Coma Scale (GCS), Simplified Acute Physiology Score II (SAPS II), Sequential Organ Failure Assessment (SOFA), and Charlson Comorbidity Index (CCI); and (5) comorbidities, such as chronic lung disease, congestive heart failure, diabetes mellitus, kidney disease, malignant cancer, severe liver disease, rheumatic disease, peripheral vascular disease, and cerebrovascular disease. All data were anonymized.

Ethical review

The MIMIC-IV database received approval from the Institutional Review Boards of Beth Israel Deaconess Medical Center and MIT. After completing the CITI Data or Specimens Only Research training, we gained access (author Jing Huang, record ID: 50199917). Patient information in the database is anonymous and de-identified, and all methods adhered to relevant guidelines and regulations.

Statistical analysis

Data are given as the mean ± SD. Figures and statistical analyses were generated using GraphPad 9.5. Comparison of means to identify differences between two groups was performed using Student's unpaired t-test. $P < 0.05$ was considered significant.

Results

Propofol inhibited the anti-C. albicans activity of neutrophils

Neutrophils were isolated from healthy volunteers following established protocols. Trypan blue staining was employed to evaluate cell viability and purity, respectively. The isolated neutrophils exhibited > 90% viability and purity (Figure S1). To assess the direct effect of propofol, neutrophils were pre-treated with or without propofol before co-culture with *C. albicans*. Propofol pretreatment caused a marked elevation in colony-forming units (CFUs), indicating a decrease in neutrophil-mediated fungal clearance, compared to the control group (**Figure 1A**, **1B**). Crystal violet staining and fungal load assays confirmed this inhibitory effect, as cultures pretreated with propofol exhibited a higher fungal burden. Furthermore, we compared the effects of propofol pretreatment on different innate immune cells and found that the inhibition of antifungal activity was only observed in neutrophils. Under the same treatment conditions, the antifungal capacities of macrophages and DCs remained unchanged (**Figures 1C-E**, S2). Significantly, propofol, at the concentrations used (0-30 μM), did not directly affect neutrophils or *C. albicans* viability, excluding effects that are nonspecific fungistatic or cytotoxic (**Figure 1F-G**). The findings suggest that propofol may impair the anti-*C. albicans* activity. Consequently, the emphasis of future research is to elaborate on the molecular mechanism of the regulation of propofol-mediated neutrophils' antifungal activity.

Propofol administration exacerbated C. albicans infection severity and reduces survival in mice

To further verify this phenomenon, we conducted preliminary in vivo experiments. In two independent trials, the mice treated with propofol showed a more pronounced trend of weight loss and reduced survival rate relative to the control group (**Figure 2A**, **2B**). As depicted in **Figure 2C**, the experimental pathology analysis showed that, in contrast to the control group, kidney sections of mice in the propofol group displayed a reduced degree of inflammation, and PAS staining results indicated an increased fungal load. ELISA assays quantified inflammatory cytokines in mice 24 hours post-infection, demonstrating significant decreases in TNF-α, IL-1β, and IL-6 levels (**Figure 2D**). On day 5, after homogenizing kidney and liver tissues, we measured cytokine concentrations in tissue supernatants. The results showed that TNF-α, IL-1β, and IL-6 levels were also significantly lower in the propofol-treated group (**Figure 2E**, **2F**). In addition, the inflammation coefficients of the spleen, liver, and kidney were measured at 24 hours and 5 days. The results showed that propofol significantly reduced the inflammation in the liver and kidney, but had no significant effect on the spleen (**Figure 2G**, **2H**). These in vivo results collectively indicate that propofol impacts the host immune response, thereby impairing immune-mediated fungal clearance.

Propofol inhibited ferroptosis in neutrophils infected with C. albicans

To elucidate the molecular mechanisms by which propofol influences neutrophils, we col-

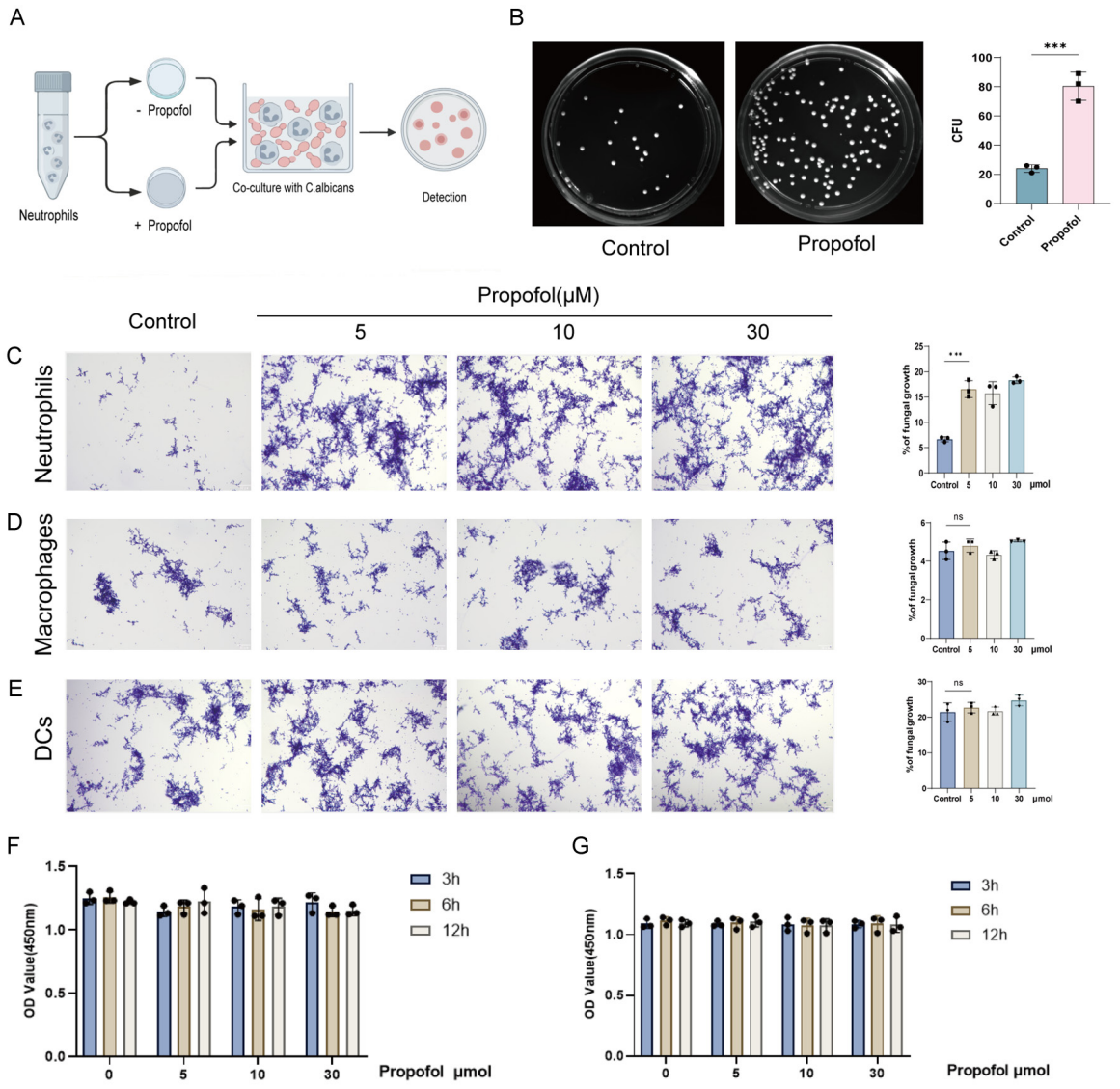

Figure 1. Propofol inhibited the anti-*C. albicans* activity of neutrophils. A. Schematic representation of the cell treatments. B. Representative images of colony-forming units (CFUs) assays are shown. Neutrophils were pretreated with propofol or without propofol then incubated with *C. albicans* (MOI = 3). Following co-culture, lysates were plated on YPD agar. Propofol treatment has markedly enhanced the CFUs as compared to control without pretreatment indicating inhibited killing of fungus. Data are representative data of three independent experiments. C-E. Neutrophils, macrophages, and DCs were pretreated with propofol at final concentrations of 5, 10, and 30 μM, followed by addition of *C. albicans* (MOI = 1:20). After overnight incubation, cells were stained with crystal violet; *Scale bar* = 200 μm. The CCK-8 assay was employed to investigate the effects of propofol at various concentrations (0, 5, 10, and 30 μM) on the activity of neutrophils (F) and *C. albicans* (G) across different time points (3, 6, and 12 h) (ns: not significant; ***$P < 0.001$).

lected human neutrophils from both a control group and a propofol-pretreated group following co-culture with *C. albicans*. Transcriptome sequencing was conducted, followed by analyses of differential gene expression and pathway enrichment. KEGG analysis revealed that the upregulated pathways in the propofol group were predominantly associated with ferroptosis. Compared to the control group, the propofol-treated group exhibited 181 upregulated and 148 downregulated genes (**Figure 3A-C**). Furthermore, Western blot analysis demonstrated that propofol treatment significantly downregulated MDA and acyl-CoA synthetase long-chain family member 4 (ACSL4) protein expression in neutrophils, while elevating gluta-

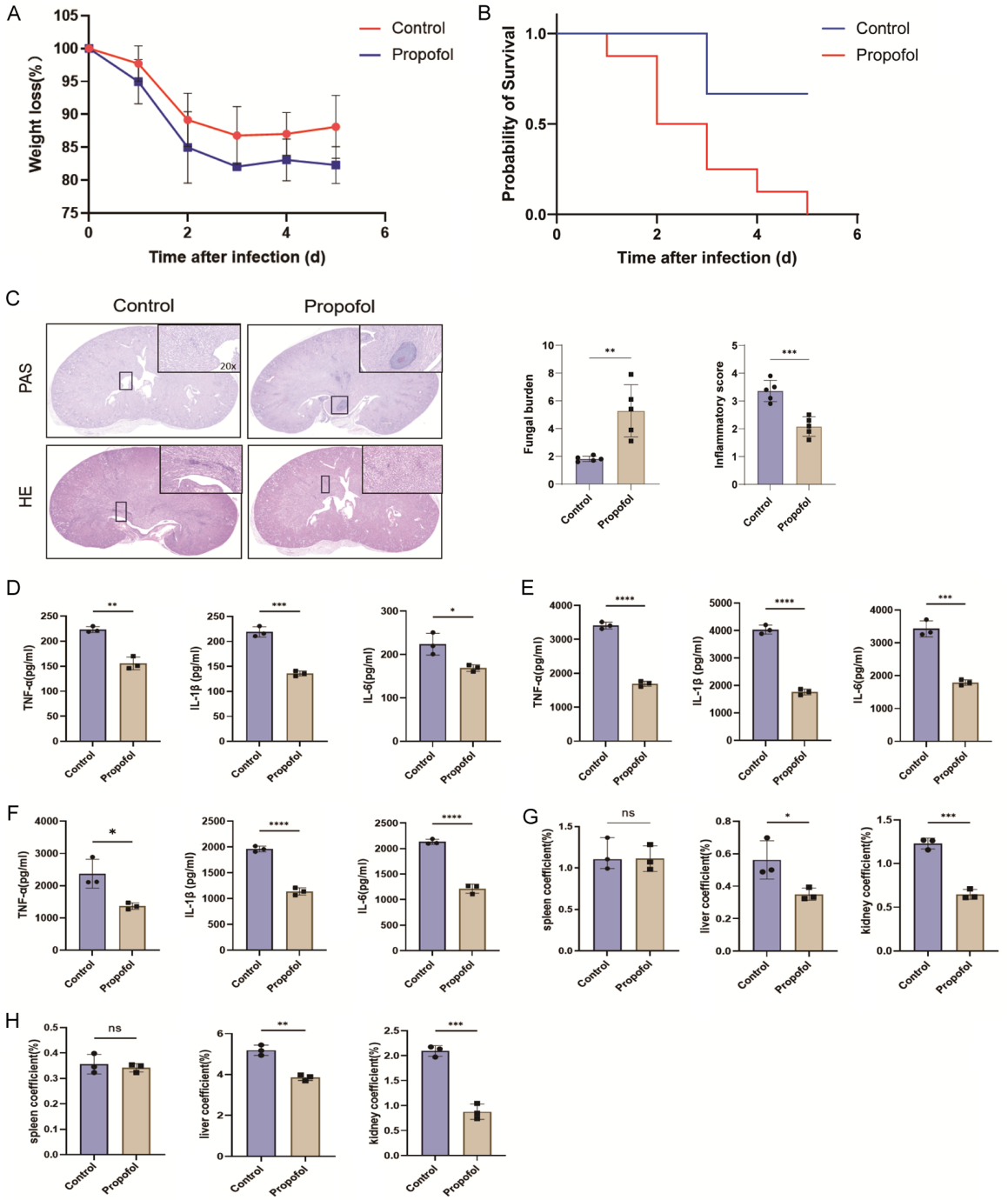

Figure 2. Propofol administration exacerbated *C. albicans* infection severity and reduces survival in mice. (A) Weight loss of mice pretreated with intraperitoneal injection of propofol (40 mg/kg) and subsequently infected with *C. albicans* (4×10^5 CFUs) via tail vein injection, compared to controls. (B) Survival curves of mice following propofol pretreatment and *C. albicans* infection (n = 12/group). (C) Five days after infection, kidney sections were stained with H&E and PAS for differences in inflammation and fungal burden between groups; *Scale bar* = 500 μm. TNF-α, IL-1β, and IL-6 levels in (D) Twenty-four hour kidney homogenates, (E) Five day kidney homogenates, and (F) Five day liver homogenates. Inflammation coefficients of the spleen, liver, and kidney were measured at (G) Twenty-four hours and (H) Five days post-infection, demonstrating the effect of propofol on tissue inflammation (ns: not significant, $*P < 0.05$, $**P < 0.01$, $***P < 0.001$, $****P < 0.0001$).

thione peroxidase 4 (GPX4) levels (**Figure 3D**, **3E**). As a key enzyme in lipid metabolism, ACSL4 promotes lipid peroxidation by catalyzing the esterification of polyunsaturated fatty

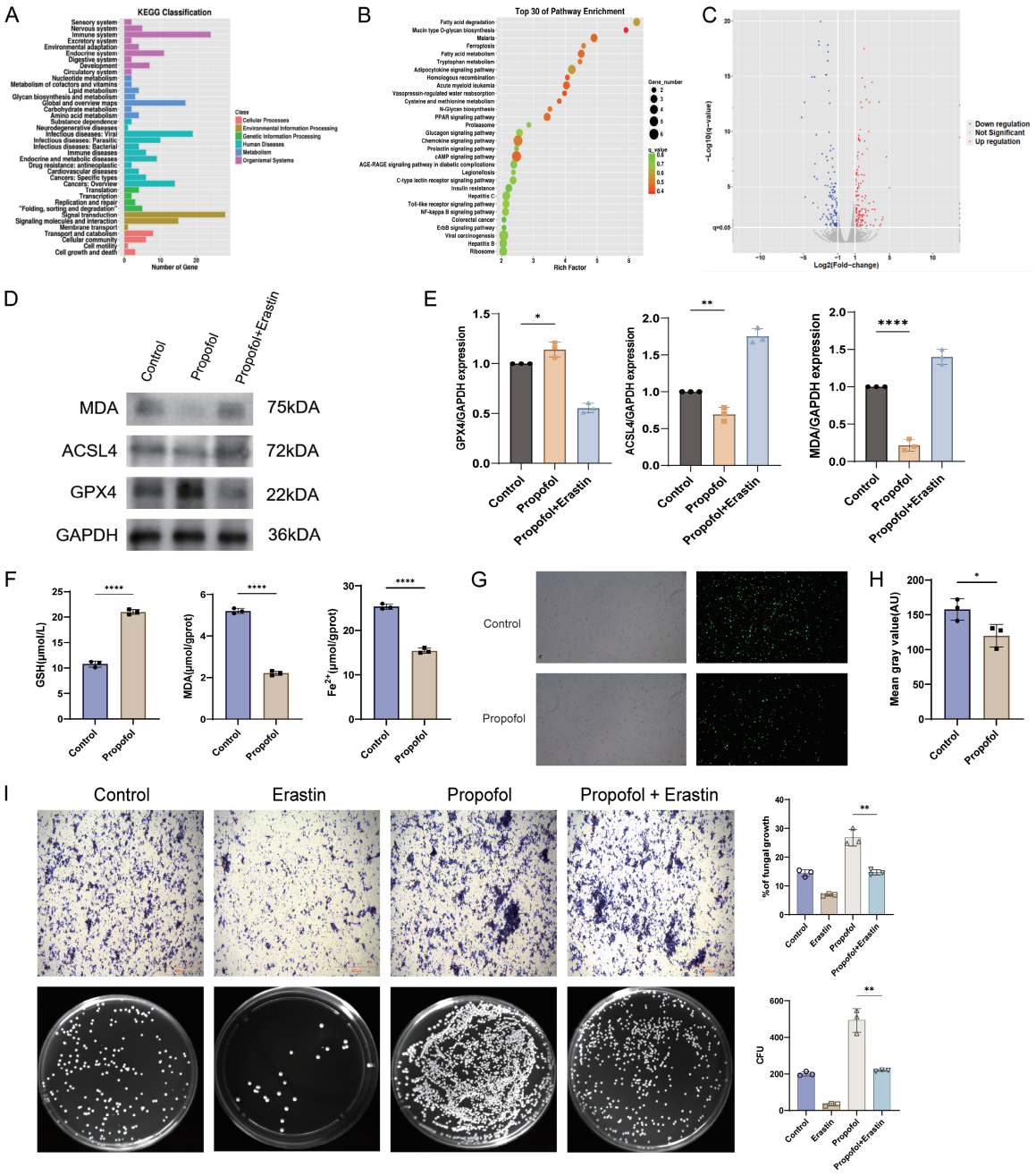

Figure 3. Propofol inhibited ferroptosis in neutrophils infected with *C. albicans*. Molecular mechanisms of propofol's effects on neutrophils. (A) KEGG pathway analysis results, (B) pathway enrichment analysis and (C) gene expression analysis outcomes, illustrated differential gene regulation in propofol-treated versus control neutrophils. (D) Western blot analysis of MDA, ACSL4, GPX4, and GAPDH protein expression in neutrophils treated with propofol. (E) Quantitative analysis of ACSL4, GPX4, and MDA protein expression normalized to GAPDH. (F) ELISA assays of GSH, MDA, and Fe^{2+} levels in neutrophils treated with propofol. (G) Representative images of intracellular lipid peroxidation fluorescence in neutrophils with propofol treatment. *Scale bar* = 200 μm. (H) Quantification of changes in fluorescence intensity. (I) Neutrophils were pretreated with PBS, Erastin, propofol or propofol plus Erastin for 1 hour, and then co-cultured with *C. albicans* (MOI = 3) for 3 hours. Fungal load was determined by colony-forming units (CFUs) or crystal violet staining. The data are expressed as the mean ± SD of three independent experiments (**P* < 0.05, ***P* < 0.01, ****P* < 0.001, *****P* < 0.0001).

acids (PUFAs), whereas GPX4 suppresses ferroptosis through the reduction of lipid peroxides. Meanwhile, propofol-treated neutrophils exhibited attenuated oxidative stress signa-

tures: significantly increased GSH concentrations accompanied by reduced MDA and Fe^{2+} levels (**Figure 3F**). These collective alterations suggest propofol-induced attenuation of ferroptosis hallmarks. Fluorescence quantification further confirmed ferroptotic suppression, as propofol treatment diminished lipid peroxidation signals in neutrophils (**Figure 3G**, **3H**). To determine whether ferroptosis inhibition directly impairs antifungal function, we conducted experiments using Erastin. It is worth noting that Erastin alone enhanced the bactericidal ability of neutrophils. Furthermore, co-treatment with Erastin significantly reversed the antifungal deficiency caused by propofol (**Figure 3I**), indicating a relationship between propofo-mediated ferroptosis inhibition and impaired fungal clearance. Collectively, these findings indicate that propofol inhibits neutrophil ferroptosis by disrupting the ACSL4/GPX4 regulatory axis and compromising redox homeostasis.

Propofol inhibited cGAS-STING signaling activation in neutrophils infected with C. albicans

Transcriptome sequencing has identified a significant upregulation of ferroptosis-related pathways. With the crucial role of the cGAS-STING pathway in antifungal immunity, we next investigated whether propofol exerts its effect by modulating this pathway in neutrophils. Western blot analysis elucidated the cGAS were significantly decreased in propofol-treated neutrophils co-cultured with HKCA (**Figure 4A**, **4B**). This suppression was similarly observed upon α-mannan stimulation (**Figure 4C**, **4D**), confirming consistent pathway inhibition across different fungal antigen triggers. These results suggested that propofol inhibits the activation of cGAS-STING signaling in neutrophils infected with *C. albicans*.

Fungemia patients on propofol in the MIMIC database experienced extended hospital stays

To explore the effect of propofol on ICU patients with fungal infections, we performed data retrieval and patient matching analysis using the MIMIC-IV database. Among 50,920 included patients, 836 had deep fungal infections: 568 received propofol treatment, while 268 did not (**Figure 5**). The study extracted clinical characteristics, laboratory results, complications, and severity scores. Sample type distribution revealed that blood samples accounted for 23%, followed by sputum (20%) and swab samples (13%) (**Figure 6A**), highlighting the diversity of specimens used for fungal detection. Regarding fungal species distribution (**Figure 6B**), *C. albicans* was the most prevalent pathogen (17%), followed by *Candida glabrata* (11%) and *Aspergillus fumigatus* (8%), consistent with previous reports identifying *C. albicans* as a major cause of invasive candidiasis in critically ill patients. All patient data were anonymized, with the study cohort aged 53-75 years (mean 54.5 years), and the average Charlson Comorbidity Index was 6 (range 4-8) (**Table 1**). Statistical analysis showed that propofol use significantly prolonged hospital stay in fungemia patients, while no significant differences were observed in other outcomes (**Table 2**).

Discussion

Over the past four decades, invasive candidiasis has evolved into a leading determinant of morbidity, mortality, and health-care expenditure in critically ill patients [34, 35]. ICU populations are characterized by profound immunoparesis and impaired barrier defenses, both of which are further compounded by multiple, often uncontrolled, predisposing factors [36]. Surgical trauma, indwelling catheters, endotracheal intubation, and central venous access collectively breach anatomical barriers and provide fungi with direct portals of entry [37]. Perioperative anesthetic management constitutes an under-recognized but potentially modifiable component of this risk landscape. Regional or local anesthetics, together with the intravenous hypnotic propofol, have been shown to preserve or even enhance peri-operative immune homeostasis [38-40]. Conversely, inhalation anesthetics, thiopental, and opioids may exert detrimental effects. By restoring immunological equilibrium, rational anesthetic strategies may attenuate ICU-acquired immunosuppression and potentiate innate cellular responses against *C. albicans* [34].

Previous studies have demonstrated that propofol exerts immunomodulatory effects, specifically impairing macrophage functions such as chemotaxis, oxidative burst, and phagocytosis [17, 41]. Additionally, propofol modulates the synthesis of pro-inflammatory cytokines in macrophages. Specifically, it has been documented that the biosynthesis of TNF-α, IL-1β,

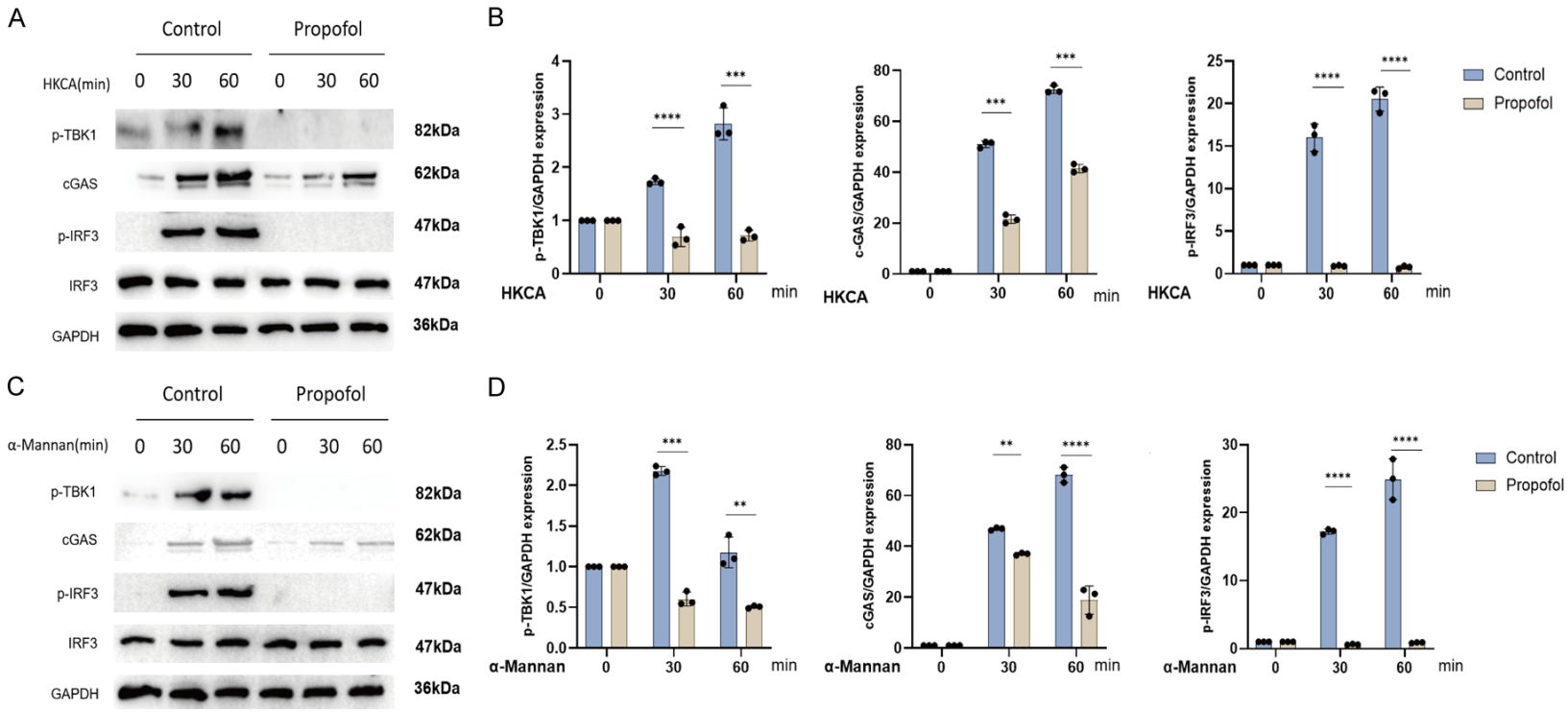

Figure 4. Propofol inhibited cGAS-STING signaling activation in neutrophils infected with *C. albicans*. A. Protein expressions of p-TBK1, c-GAS, and p-IRF3 at 0, 30, and 60minutes post HKCA treatment via Western Blot analysis. B. Quantification of p-TBK1, c-GAS, and p-IRF3 protein expression after HKCA treatment. C. Protein expressions of p-TBK1, c-GAS, and p-IRF3 at 0, 30, and 60 minutes post α-Mannan treatment via Western Blot analysis. D. Quantification of p-TBK1, c-GAS, and p-IRF3 protein expression after α-Mannan treatment (***P* < 0.01, ****P* <0.001, *****P* < 0.0001).

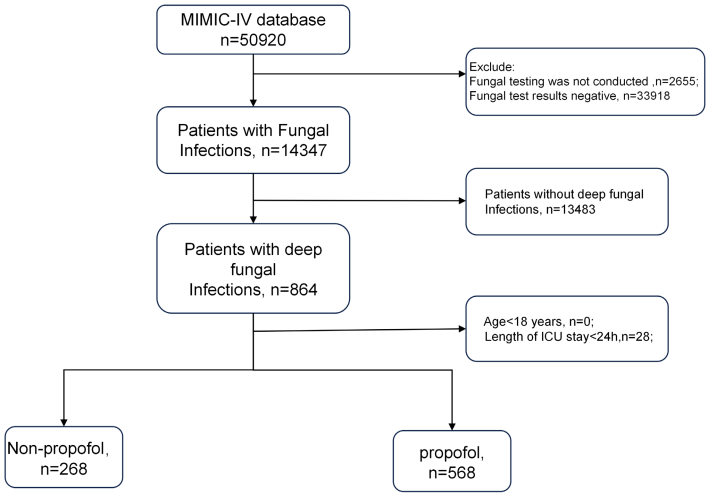

Figure 5. Flowchart of patient screening.

and IL-6 is inhibited in lipopolysaccharide (LPS)-activated macrophages when treated with propofol at therapeutic concentrations [18]. Furthermore, excessive administration of propofol in macrophages has been demonstrated to inhibit phagocytosis and induce apoptosis [42-44]. However, the influence of propofol on the antifungal activity of neutrophils against *C. albicans* remains underexplored.

In this study, we conducted a preliminary investigation into the potential negative regulatory effects of propofol on the antifungal immunity of neutrophils. Initially, we employed crystal violet staining and colony plate counting to compare colony counts between the control group and the propofol-treated group. The results demonstrated a significant increase in colony numbers in the propofol-treated group, independent of the direct influence of the drug itself. Subsequently, we performed in vivo experiments utilizing a *C. albicans* infection model in C57BL/6 mice to further elucidate these findings. The results demonstrated that compared to the control group, the propofol-treated group exhibited more severe renal inflammation, characterized by neutrophil infiltration. Additionally, PAS staining revealed an increased fungal burden in the propofol group, with a marked difference compared to the control group. This suggests that propofol may have caused excessive inflammatory suppression that inhibited the ability of the immune system to kill *C. albicans*, thereby inhibiting the immune system's ability to kill *C. albicans*.

Furthermore, ELISA analysis of murine models revealed significantly decreased concentrations of TNF-α, IL-1β, and IL-6 in propofol-pretreated groups. To elucidate the underlying mechanisms, we conducted RNA sequencing followed by Western blot validation. Our findings demonstrate that propofol primarily impairs neutrophil-mediated clearance of *C. albicans* by inhibiting ferroptosis pathways. Analysis of MIMIC-IV clinical data corroborated these results, showing prolonged hospitalization in propofol-treated patients, suggesting compromised antifungal immunity during *C. albicans* infection. Critically, the causal role of ferroptosis inhibition in the immunosuppressive effects of propofol was functionally validated by rescue experiments. We found that Erastin not only enhanced the fungicidal capacity of neutrophils by itself, but more importantly, it significantly reversed the propofol induced antifungal defect, directly proving that inhibition of ferroptosis is the primary mechanism driving impaired clearance of *C. albicans*.

Overall, this study does have some limitations. While this study mechanistically demonstrated that propofol impairs the antifungal function of neutrophils by inhibiting the cGAS-STING pathway and suppressing ferroptosis, as evidenced by in vitro experiments, animal models, and clinical data analysis, further research is required to establish a causal relationship and to enhance the specificity of the underlying mechanism. Future work will exclude potential interference from alternative cell death pathways and definitively confirm whether ferroptosis represents the primary mechanism of propofol action. Due to the limited sample size in the animal study, no formal statistical analysis was conducted on the changes in mouse weight and survival; however, the observed trend indicates that a more statistically robust in vivo study is necessary to confirm these effects. Moreover, while clinical data associate propofol exposure with prolonged hospitalization in fungal-infected patients, heterogeneity in ICU cohorts, including variability in mechanical ventilation duration and concomitant medications, may introduce confounding factors. Prospective

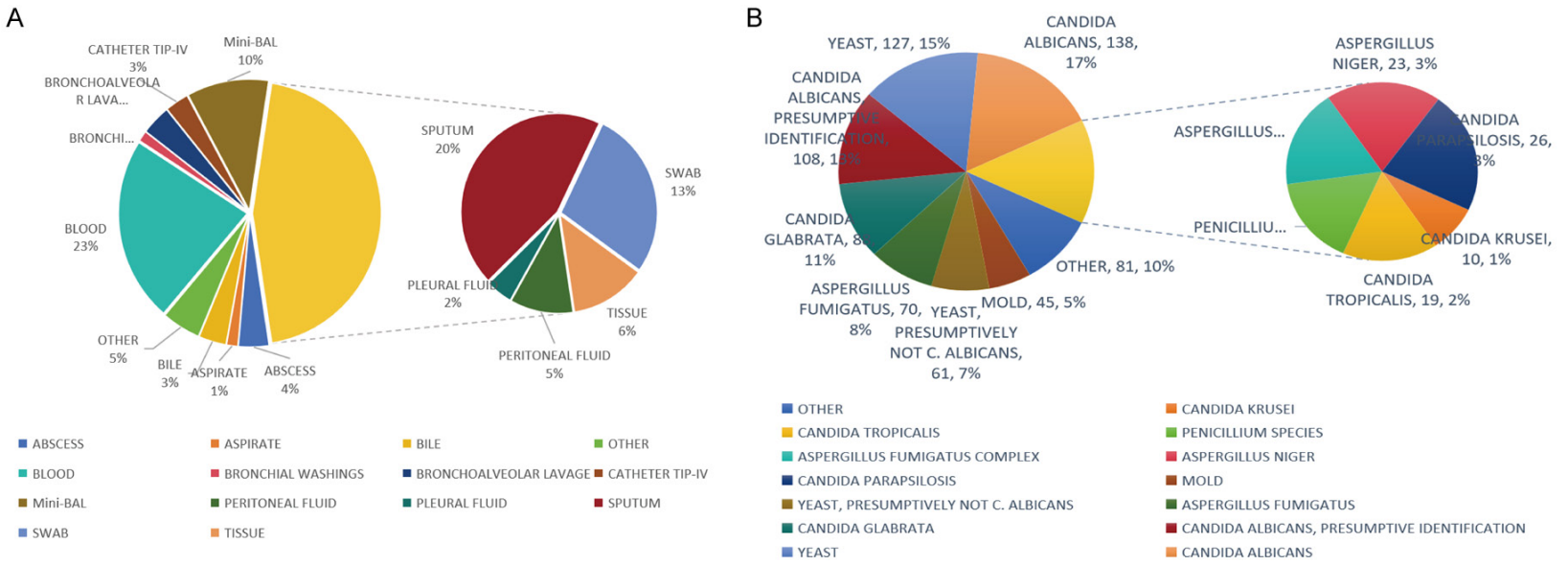

Figure 6. Distribution of sample types and fungal species in the MIMIC-IV database. A. Distribution of the proportion of different samples in the test. Blood samples constituted 23% of total specimens, followed by sputum samples at 20% and swab samples at 13%. B. The distribution of different fungal species. *C. albicans* was the most common (17%), followed by *Candida glabrata* (11%) and *Aspergillus fumigatus* (8%).

Table 1. Baseline characteristics

Patient characteristics	Non-propofol	Propofol	*P*-Value
Age (year)	66.8 (54.5-77.4)	65.0 (53.4-74.8)	0.071
BUN (mg/dL)	29.5 (18.0-54.8)	29.0 (18.0-46.0)	0.623
Charlson comorbidity score	6.0 (4.0-8.0)	6.0 (4.0-8.0)	0.436
Central Nervous System (CNS) infection severity score	1.0 (1.0-3.0)	3.0 (1.0-4.0)	< 0.01
Creatinine (mg/dL)	1.3 (0.8-2.5)	1.4 (0.9-2.5)	0.151
Glasgow Coma Scale (GCS) Scores	13.0 (9.0-14.0)	9.0 (3.3-14.0)	< 0.01
Maximum heart rate	111.5 (96.0-129.0)	114.5 (98.0-130.0)	0.203
Height (cm)	168.0 (160.5-176.8)	170.0 (161.0-178.0)	0.260
HbAb (μg/mL)	8.9 (7.9-10.5)	9.0 (7.9-10.5)	0.987
Lactic acid (mmol/L)	2.1 (1.6-3.3)	2.6 (1.7-4.8)	< 0.01
Minimum Values of Mean Arterial Pressure (mmHg)	54.0 (47.0-63.0)	56.0 (48.0-62.0)	0.373
Minimum Values of pCO_2 (mmHg)	43.0 (39.0-49.0)	48.1 (41.0-58.8)	< 0.01
Minimum Values of pH	7.36 (7.26-7.41)	7.28 (7.19-7.37)	< 0.01
Minimum Values of Platelets (10^9/L)	193.0 (107.0-302.3)	155.0 (84.0-234.0)	< 0.01
Minimum Values of pO_2 (mmHg)	63.0 (41.0-85.8)	60.0 (42.0-88.8)	0.842
Maximum Values of Respiratory Rate (breaths/min)	28.0 (25.0-34.0)	30.0 (26.0-34.0)	0.198
SAPSII score	41.0 (31.0-53.0)	46.0 (37.0-56.8)	< 0.01
SOFA score	7.0 (4.0-10.0)	10.0 (7.0-13.0)	< 0.01
Minimum Values of Oxygen Partial Pressure (mmHg)	92.0 (89.0-94.0)	92.0 (88.0-95.0)	0.116
Maximum Value of Body Temperature (°C)	37.3 (36.9-38.1)	37.6 (37.1-38.3)	0.004
Urine Volume (mL/24 h)	1223.5 (605.5-2068.8)	1155.0 (585.0-1895.3)	0.304
WBCs (10^9/L)	15.2 (9.4-22.4)	16.0 (11.2-22.2)	0.122
Weight (kg)	78.2 (62.9-94.1)	81.6 (67.1-97.4)	0.105

Note: BUN: Blood urea nitrogen; HbAb: Hemoglobin Antibody; SAPSII score: Simplified Acute Physiology Score II; SOFA score: Sequential Organ Failure Assessment.

Table 2. Outcomes in patients with or without propofol administration following fungal infection

Outcome	Non-propofol	Propofol	*P-Value*
7-day mortality	44/233 (18.9%)	36/233 (15.5%)	0.326
14-day mortality	75/233 (32.2%)	64/233 (27.5%)	0.266
30-day mortality	101/233 (43.3%)	95/233 (40.8%)	0.574
90-day mortality	127/233 (54.5%)	111/233 (47.6%)	0.139
ICU mortality	75/233 (32.2%)	77/233 (33.0%)	0.844
Hospital mortality	88/233 (37.8%)	90/233 (38.6%)	0.849
Total in-hospital stay	13.0 (7.1-21.2)	14.3 (8.7-21.9)	0.243
Total ICU stay	7.3 (4.4-11.8)	9.3 (4.8-14.0)	0.032

cohort studies or conditional knockout models should be implemented to validate the clinical relevance of this association.

In conclusion, our study has preliminarily demonstrated that propofol inhibits the neutrophil-mediated killing of *C. albicans* both in vitro and in vivo. We have established that propofol suppresses neutrophil antifungal activity against *C. albicans*, which may provide valuable insights for drug recommendations in ICU patients with fungal infections.

Acknowledgements

The authors disclose receipt of the following support for the research, authorship, and/or publication of this article: This work was supported by National Natural Science Foundation of China (Grant Nos. 82202584, 82372313), Program of Shanghai Academic/Technology Research Leader (Grant No. 23XD-1404900), and Shanghai Science and Technology Committee under Grant (Grant No. 21ZR1478200).

Disclosure of conflict of interest

None.

Address correspondence to: Lin Zhou, Department of Laboratory Medicine, Shanghai Changzheng Hospital, Naval Medical University, 415 Fengyang Road,

Shanghai 200003, China. E-mail: lynnzhou36@126.com; Liangqing Lin, Department of Anesthesiology, The First Hospital of Putian City, Teaching Hospital of Fujian Medical University, 449 Nanmen West Road, Putian, 351100, Fujian, China. E-mail: linliangqing2021@outlook.com; Ning Ma, Department of Clinical Laboratory, 905th Hospital of PLA, Shanghai 200052, China. E-mail: mamimg@sina.com

References

[1] Li J, Hirota K, Goto T, Yumoto H, Miyake Y and Ichikawa T. Biofilm formation of Candida albicans on implant overdenture materials and its removal. J Dent 2012; 40: 686-692.

[2] Achkar JM and Fries BC. Candida infections of the genitourinary tract. Clin Microbiol Rev 2010; 23: 253-273.

[3] Ponde NO, Lortal L, Ramage G, Naglik JR and Richardson JP. Candida albicans biofilms and polymicrobial interactions. Crit Rev Microbiol 2021; 47: 91-111.

[4] Kullberg BJ and Arendrup MC. Invasive Candidiasis. N Engl J Med 2015; 373: 1445-1456.

[5] Dantas Ada S, Day A, Ikeh M, Kos I, Achan B and Quinn J. Oxidative stress responses in the human fungal pathogen, Candida albicans. Biomolecules 2015; 5: 142-165.

[6] Austermeier S, Kasper L, Westman J and Gresnigt MS. I want to break free - macrophage strategies to recognize and kill Candida albicans, and fungal counter-strategies to escape. Curr Opin Microbiol 2020; 58: 15-23.

[7] Iwasaki A and Medzhitov R. Regulation of adaptive immunity by the innate immune system. Science 2010; 327: 291-295.

[8] Medzhitov R and Janeway C Jr. Innate immunity. N Engl J Med 2000; 343: 338-344.

[9] Banchereau J and Steinman RM. Dendritic cells and the control of immunity. Nature 1998; 392: 245-252.

[10] Gordon S. Alternative activation of macrophages. Nat Rev Immunol 2003; 3: 23-35.

[11] Nathan C. Neutrophils and immunity: challenges and opportunities. Nat Rev Immunol 2006; 6: 173-182.

[12] Vivier E, Raulet DH, Moretta A, Caligiuri MA, Zitvogel L, Lanier LL, Yokoyama WM and Ugolini S. Innate or adaptive immunity? The example of natural killer cells. Science 2011; 331: 44-49.

[13] Dinarello CA. Historical insights into cytokines. Eur J Immunol 2007; 37 Suppl 1: S34-S45.

[14] Brinkmann V, Reichard U, Goosmann C, Fauler B, Uhlemann Y, Weiss DS, Weinrauch Y and Zychlinsky A. Neutrophil extracellular traps kill bacteria. Science 2004; 303: 1532-1535.

[15] Borregaard N. Neutrophils, from marrow to microbes. Immunity 2010; 33: 657-670.

[16] Acartürk TO. Free segmental vastus lateralis muscle flap for reconstruction of recalcitrant defects of the cleft hard palate. J Reconstr Microsurg 2012; 28: 509-514.

[17] Hsu HT, Tseng YT, Hsu YY, Cheng KI, Chou SH and Lo YC. Propofol attenuates lipopolysaccharide-induced reactive oxygen species production through activation of Nrf2/GSH and suppression of NADPH oxidase in human alveolar epithelial cells. Inflammation 2015; 38: 415-423.

[18] Sun L, Ma W, Gao W, Xing Y, Chen L, Xia Z, Zhang Z and Dai Z. Propofol directly induces caspase-1-dependent macrophage pyroptosis through the NLRP3-ASC inflammasome. Cell Death Dis 2019; 10: 542.

[19] Liu D, Liang C-H, Huang B, Zhuang X, Cui W, Yang L, Yang Y, Zhang Y, Fu X, Zhang X, Du L, Gu W, Wang X, Yin C, Chai R and Chu B. Tryptophan metabolism acts as a new anti-ferroptotic pathway to mediate tumor growth. Adv Sci (Weinh) 2023; 10: e2204006.

[20] Luo Y, Apaijai N, Liao S, Maneechote C, Chunchai T, Arunsak B, Benjanuwattra J, Yanpiset P, Chattipakorn SC and Chattipakorn N. Therapeutic potentials of cell death inhibitors in rats with cardiac ischaemia/reperfusion injury. J Cell Mol Med 2022; 26: 2462-2476.

[21] Stockwell BR, Friedmann Angeli JP, Bayir H, Bush AI, Conrad M, Dixon SJ, Fulda S, Gascon S, Hatzios SK, Kagan VE, Noel K, Jiang X, Linkermann A, Murphy ME, Overholtzer M, Oyagi A, Pagnussat GC, Park J, Ran Q, Rosenfeld CS, Salnikow K, Tang D, Torti FM, Torti SV, Toyokuni S, Woerpel KA and Zhang DD. Ferroptosis: a regulated cell death nexus linking metabolism, redox biology, and disease. Cell 2017; 171: 273-285.

[22] Vandenabeele P, Galluzzi L, Vanden Berghe T and Kroemer G. Molecular mechanisms of necroptosis: an ordered cellular explosion. Nat Rev Mol Cell Biol 2010; 11: 700-714.

[23] Muñoz VL, Porsch EA and St Geme JW 3rd. Kingella kingae Surface Polysaccharides Promote Resistance to Neutrophil Phagocytosis and Killing. mBio 2019; 10: e00631-19.

[24] Kolaczkowska E and Kubes P. Neutrophil recruitment and function in health and inflammation. Nat Rev Immunol 2013; 13: 159-175.

[25] Scapini P and Cassatella MA. Social networking of human neutrophils within the immune system. Blood 2014; 124: 710-719.

[26] Stockwell BR and Jiang X. A physiological function for ferroptosis in tumor suppression by the immune system. Cell Metab 2019; 30: 14-15.

[27] Millet N, Solis NV, Aguilar D, Lionakis MS, Wheeler RT, Jendzjowsky N and Swidergall M. IL-23 signaling prevents ferroptosis-driven renal immunopathology during candidiasis. Nat Commun 2022; 13: 5545.

[28] Zhu CL, Xie J, Liu Q, Wang Y, Li HR, Yu CM, Li P, Deng XM, Bian JJ and Wang JF. PD-L1 promotes GSDMD-mediated NET release by maintaining the transcriptional activity of Stat3 in sepsis-associated encephalopathy. Int J Biol Sci 2023; 19: 1413-1429.
[29] Loh JT, Xu S, Huo JX, Kim SS, Wang Y and Lam KP. Dok3-protein phosphatase 1 interaction attenuates Card9 signaling and neutrophil-dependent antifungal immunity. J Clin Invest 2019; 129: 2717-2729.
[30] Han F, Guo H, Wang L, Zhang Y, Sun L, Dai C and Wu X. The cGAS-STING signaling pathway contributes to the inflammatory response and autophagy in Aspergillus fumigatus keratitis. Exp Eye Res 2020; 202: 108366.
[31] Wang X, Zhang H, Shao Z, Zhuang W, Sui C, Liu F, Chen X, Hou J, Kong L, Liu H, Zheng Y, Liu B, Chen T, Zhang L, Jia X and Gao C. TRIM31 facilitates K27-linked polyubiquitination of SYK to regulate antifungal immunity. Signal Transduct Target Ther 2021; 6: 298.
[32] Zhu CL, Xie J, Liu Q, Wang Y, Li HR, Yu CM, Li P, Deng XM, Bian JJ and Wang JF. PD-L1 promotes GSDMD-mediated NET release by maintaining the transcriptional activity of Stat3 in sepsis-associated encephalopathy. Int J Biol Sci 2023; 19: 1413-1429.
[33] Loh JT, Xu S, Huo JX, Kim SS, Wang Y and Lam KP. Dok3-protein phosphatase 1 interaction attenuates Card9 signaling and neutrophil-dependent antifungal immunity. J Clin Invest 2019; 129: 2717-2729.
[34] Dadar M, Tiwari R, Karthik K, Chakraborty S, Shahali Y and Dhama K. Candida albicans - Biology, molecular characterization, pathogenicity, and advances in diagnosis and control - An update. Microb Pathog 2018; 117: 128-138.
[35] Soulountsi V, Schizodimos T and Kotoulas SC. Deciphering the epidemiology of invasive candidiasis in the intensive care unit: is it possible? Infection 2021; 49: 1107-1131.
[36] van Vught LA, Wiewel MA, Hoogendijk AJ, Frencken JF, Scicluna BP, Klein Klouwenberg PMC, Zwinderman AH, Lutter R, Horn J, Schultz MJ, Bonten MMJ, Cremer OL and van der Poll T. The host response in patients with sepsis developing intensive care unit-acquired secondary infections. Am J Respir Crit Care Med 2017; 196: 458-470.
[37] Esper AM and Martin GS. The impact of comorbid [corrected] conditions on critical illness. Crit Care Med 2011; 39: 2728-2735.
[38] Hu C, Iwasaki M, Liu Z, Wang B, Li X, Lin H, Li J, Li JV, Lian Q and Ma D. Lung but not brain cancer cell malignancy inhibited by commonly used anesthetic propofol during surgery: Implication of reducing cancer recurrence risk. J Adv Res 2021; 31: 1-12.
[39] Xu ZZ, Li HJ, Li MH, Huang SM, Li X, Liu QH, Li J, Li XY, Wang DX and Sessler DI. Epidural anesthesia-analgesia and recurrence-free survival after lung cancer surgery: a randomized trial. Anesthesiology 2021; 135: 419-432.
[40] Sekandarzad MW, van Zundert AAJ, Lirk PB, Doornebal CW and Hollmann MW. Perioperative anesthesia care and tumor progression. Anesth Analg 2017; 124: 1697-1708.
[41] Kurosawa S and Kato M. Anesthetics, immune cells, and immune responses. J Anesth 2008; 22: 263-277.
[42] Krumholz W, Endrass J and Hempelmann G. Propofol inhibits phagocytosis and killing of Staphylococcus aureus and Escherichia coli by polymorphonuclear leukocytes in vitro. Can J Anaesth 1994; 41: 446-449.
[43] Chen RM, Wu CH, Chang HC, Wu GJ, Lin YL, Sheu JR and Chen TL. Propofol suppresses macrophage functions and modulates mitochondrial membrane potential and cellular adenosine triphosphate synthesis. Anesthesiology 2003; 98: 1178-1185.
[44] Hsing CH, Chen YH, Chen CL, Huang WC, Lin MC, Tseng PC, Wang CY, Tsai CC, Choi PC and Lin CF. Anesthetic propofol causes glycogen synthase kinase-3β-regulated lysosomal/mitochondrial apoptosis in macrophages. Anesthesiology 2012; 116: 868-881.

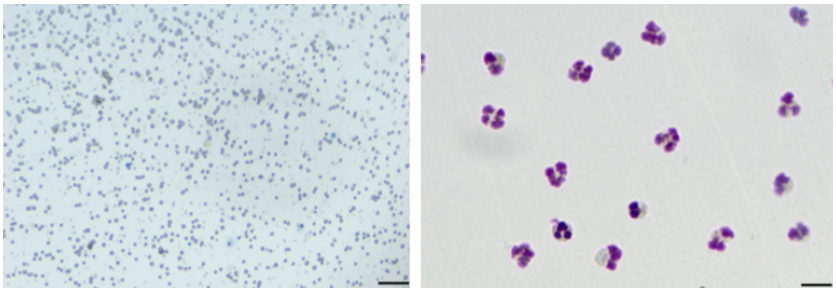

Figure S1. Trypan blue (left) and Giemsa (right) staining were used to detect the activity and purity of extracted primary cells. *Scale bar* = 100 μm (left) and 20 μm (right).

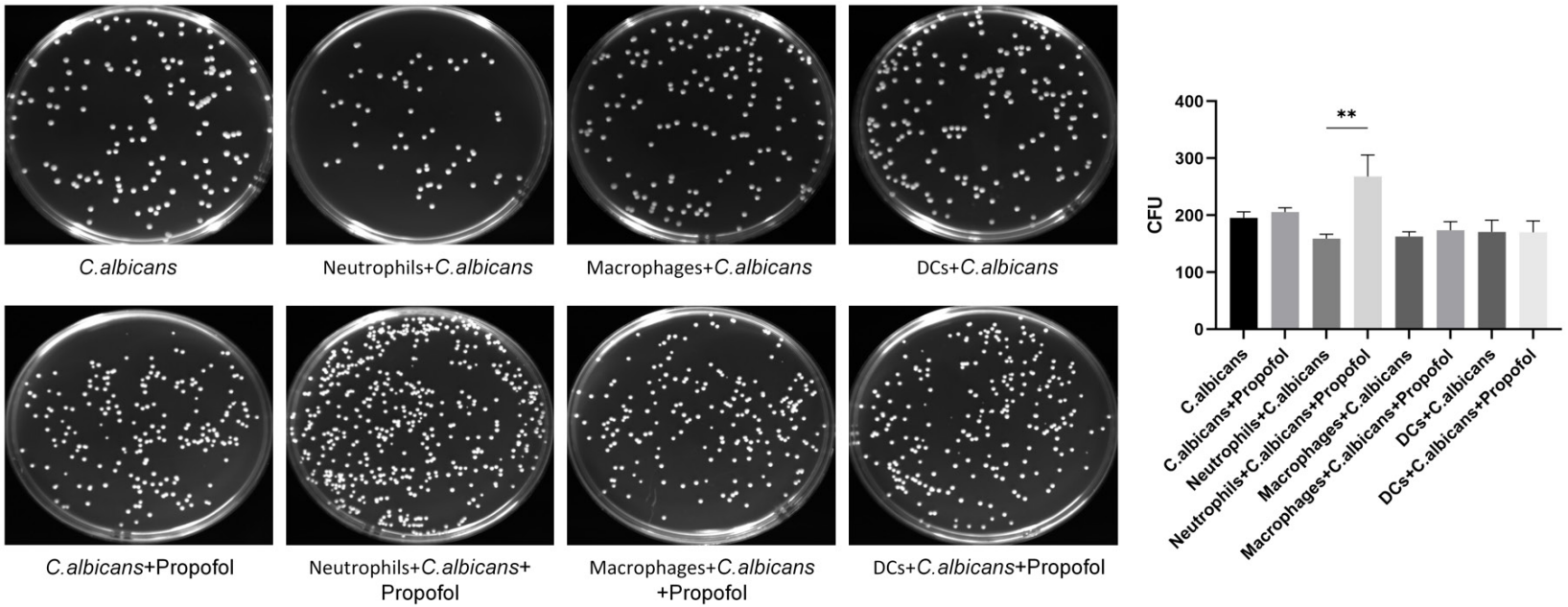

Figure S2. Assessment of effects of propofol on different innate immune cell types. Fungal load was determined by quantifying colony-forming units (CFUs). Data are presented as the mean ± SD from three independent experiments (***P < 0.01*).